

Elastic proton-neutron and antiproton-neutron scattering in holographic QCD

Akira Watanabe,^{1,2,*} Sayed Anwar Sirat,^{1,†} and Zhibo Liu^{1,‡}

¹*College of Science, China Three Gorges University,
Yichang 443002, People's Republic of China*

²*Center for Astronomy and Space Sciences, China Three Gorges University,
Yichang 443002, People's Republic of China*

(Dated: March 29, 2024)

arXiv:2305.06700v3 [hep-ph] 28 Mar 2024

Abstract

The total and differential cross sections of the elastic proton-neutron and antiproton-neutron scattering are studied in a holographic QCD model, focusing on the Regge regime. Taking into account the Pomeron and Reggeon exchange, which are described by the Reggeized spin-2 glueball and vector meson propagator respectively, those cross sections are obtained. It is presented that the currently available experimental data of the total cross sections can be well described within the model. Once a single adjustable parameter is determined with the total cross section data, the differential cross sections can be calculated without any additional parameters. Although the available differential cross section data are limited, it is found that our predictions are consistent with those.

I. INTRODUCTION

High energy elastic hadron-hadron scattering has played an important role in improving our knowledge of the strong interaction for several decades. Its cross sections shall, in principle, be described by QCD, but perturbative calculations are only available in some quite limited kinematic region, such as the high energy limit [1–3], due to the nonperturbative nature of the involved quark-gluon dynamics, which is the reason why in most kinematic regions effective approaches are basically needed. The theoretical analysis for the forward scattering is especially difficult, since the underlying partonic dynamics is highly nonperturbative. Historically, it is known that those cross sections can be well described by the Pomeron and Reggeon exchange, which can be interpreted as the multi-gluon and meson exchange, respectively. Donnachie and Landshoff first showed that experimental data of various hadron-hadron total cross sections can be well reproduced with this description [4]. The Pomeron and Reggeon exchange can also be realized in the framework of holographic QCD, and in this work we apply this to the analysis of the elastic proton-neutron (pn) and antiproton-neutron ($\bar{p}n$) scattering.

Holographic QCD [5–12] is an effective approach to QCD, which has been constructed based on the anti-de Sitter/conformal field theory (AdS/CFT) correspondence [13–15]. This

* watanabe@ctgu.edu.cn (Corresponding author)

† anwarsirat7@gmail.com

‡ 202107020021014@ctgu.edu.cn

method has served as a useful tool to perform analysis for the nonperturbative physical quantities, and has been successfully applied to studies of the spectrum and structure of hadrons [16–26]. Applications to various high energy scattering processes have also been intensively done, and a lot of successful results have been obtained so far [27–41]. In particular, in Ref. [41] the cross sections of the elastic proton-proton (pp) and proton-antiproton ($p\bar{p}$) scattering were investigated, considering the Pomeron and Reggeon exchange in holographic QCD, and it was shown that the experimental data can be well described in a wide kinematic region.

The present work is an extension of Ref. [41], and we apply the framework to study the total and differential cross sections of the pn and $\bar{p}n$ scattering, focusing on the Regge regime, in which the condition $s \gg |t|$ (s and t are the Mandelstam variables) is satisfied. The Pomeron and Reggeon exchange are described by the Reggeized spin-2 glueball and vector meson propagator, respectively. The Pomeron-nucleon couplings are described by the nucleon gravitational form factor, which can be obtained with the bottom-up AdS/QCD model [21]. The model includes several parameters which should be determined with experimental data, but considering the universality of the Pomeron and Reggeon, part of the parameter set obtained in Ref. [41] can directly be employed in this study.

It is known that the isospin symmetry between the proton and neutron is a particularly good symmetry, which can be seen by the fact that the mass difference between these particles is surprisingly small. However, since the charge difference affects the Reggeon-nucleon couplings, the Reggeon-neutron coupling constant needs to be newly determined, which can be made with the experimental data of the pn total cross section. Once this coupling constant is determined, the differential cross sections can be calculated without any additional parameters. We present that the total cross section data can be well described within the model and our predictions for the differential cross section are also consistent with the data. Since the Pomeron contribution becomes dominant as the energy increases, it is expected that the differences between the pn and $\bar{p}n$ cross sections may decrease. This behavior is explicitly shown for both the total and differential cross sections.

This paper is organized as follows. In the next section, we introduce the model setup which describes the elastic pn and $\bar{p}n$ scattering in the Regge regime. We explain how to deal with the parameters involved in the model, and present our numerical results for the total and differential cross sections in Sec. III. Finally, the conclusion of this work is given

in Sec. IV.

II. MODEL SETUP

In this study we investigate the elastic pn and $\bar{p}n$ scattering in the Regge regime, taking into account the Pomeron and Reggeon exchange. Following the preceding study [41], here we introduce expressions for the total and differential cross section. The Pomeron and Reggeon exchange can be described by the Reggeized spin-2 glueball and vector meson propagator, respectively. Since we can consider these contributions separately, the total scattering amplitudes are written as

$$\mathcal{A}_{\text{tot}}^{pn(\bar{p}n)} = \mathcal{A}_g^{pn(\bar{p}n)} + \mathcal{A}_v^{pn(\bar{p}n)}. \quad (1)$$

Considering the two-body scattering process, $1(p_1) + 2(p_2) \rightarrow 3(p_3) + 4(p_4)$, in the Regge limit the massive spin-2 glueball propagator is given by [42]

$$D_{\alpha\beta\gamma\delta}^g(k) = \frac{-i}{2(k^2 + m_g^2)} (\eta_{\alpha\gamma}\eta_{\beta\delta} + \eta_{\alpha\delta}\eta_{\beta\gamma}), \quad (2)$$

where $k = p_3 - p_1$ and m_g is the glueball mass. The glueball-nucleon-nucleon vertex in the Regge limit is given by

$$\Gamma_g^{\mu\nu} = \frac{\lambda_g A(t)}{2} (\gamma^\mu P^\nu + \gamma^\nu P^\mu), \quad (3)$$

where $P = (p_1 + p_3)/2$, $t = -k^2$, and λ_g is the coupling constant which represents the strength of the glueball-nucleon coupling. $A(t)$ is the nucleon form factor, which will be specified later. The vector meson propagator and vector-nucleon-nucleon vertex are written as

$$D_{\mu\nu}^v(k) = \frac{i}{k^2 + m_v^2} \eta_{\mu\nu}, \quad (4)$$

$$\Gamma_v^\mu = -i\lambda_v \gamma^\mu, \quad (5)$$

respectively, where m_v is the vector meson mass, and λ_v is the coupling constant which represents the strength of the vector meson-nucleon coupling.

The scattering amplitudes for the glueball and vector meson exchange can be expressed as

$$\mathcal{A}_g^{pn(\bar{p}n)} = (\bar{u}_1 \Gamma_g^{\alpha\beta} u_3) D_{\alpha\beta\gamma\delta}^g(k) (\bar{u}_2 \Gamma_g^{\gamma\delta} u_4), \quad (6)$$

$$\mathcal{A}_v^{pn(\bar{p}n)} = (\bar{u}_1 \Gamma_v^\mu u_3) D_{\mu\nu}^v(k) (\bar{u}_2 \Gamma_v^\nu u_4), \quad (7)$$

respectively, where \bar{u} and u are the nucleon spinors. Since $s \gg |t|$, $u_1 \approx u_3$, and $u_2 \approx u_4$, the differential cross section can be obtained as

$$\begin{aligned} \frac{d\sigma}{dt} &= \frac{1}{16\pi s^2} |\mathcal{A}_{\text{tot}}^{pn(\bar{p}n)}|^2 \\ &= \frac{\lambda_g^4 s^2 A^4(t)}{16\pi |t - m_g^2|^2} - \frac{\lambda_g^2 \lambda_v^2 A^2(t) s}{8\pi} \left[\frac{1}{(t - m_g^2)^*} \times \frac{1}{t - m_v^2} + \frac{1}{(t - m_v^2)^*} \times \frac{1}{t - m_g^2} \right] + \frac{\lambda_v^4}{4\pi |t - m_v^2|^2}, \end{aligned} \quad (8)$$

where the asterisk indicates complex conjugation.

Since this equation only describes the exchange of the lightest states, the both propagators need to be Reggeized to include contributions from the higher spin states on the Regge trajectories. Following the Reggeization procedure explained in detail in Ref. [43], the spin-2 glueball propagator needs to be replaced with

$$\frac{1}{t - m_g^2} \rightarrow \frac{\alpha'_g}{2} e^{-\frac{i\pi\alpha_g(t)}{2}} \left(\frac{\alpha'_g s}{2} \right)^{\alpha_g(t)-2} \frac{\Gamma\left[3 - \frac{\chi_g}{2}\right] \Gamma\left[1 - \frac{\alpha_g(t)}{2}\right]}{\Gamma\left[2 - \frac{\chi_g}{2} + \frac{\alpha_g(t)}{2}\right]}, \quad (9)$$

where $\chi_g \equiv \alpha_g(s) + \alpha_g(u) + \alpha_g(t)$ in which $\alpha_g(x) = \alpha_g(0) + \alpha'_g x$. $\alpha_g(0)$ and α'_g correspond to the Pomeron intercept and slope, respectively. On the other hand, the vector meson propagator needs to be replaced with

$$\frac{1}{t - m_v^2} \rightarrow \alpha'_v e^{-\frac{i\pi\alpha_v(t)}{2}} \sin\left[\frac{\pi\alpha_v(t)}{2}\right] (\alpha'_v s)^{\alpha_v(t)-1} \Gamma[-\alpha_v(t)], \quad (10)$$

where $\alpha_v(t) = \alpha_v(0) + \alpha'_v t$.

Therefore, the differential cross section which includes contributions from the higher spin states can be obtained as

$$\begin{aligned} \frac{d\sigma}{dt} &= \frac{\lambda_g^4 s^2 A^4(t)}{16\pi} \left[\frac{\alpha'_g}{2} \frac{\Gamma\left[3 - \frac{\chi_g}{2}\right] \Gamma\left[1 - \frac{\alpha_g(t)}{2}\right]}{\Gamma\left[2 - \frac{\chi_g}{2} + \frac{\alpha_g(t)}{2}\right]} \left(\frac{\alpha'_g s}{2} \right)^{\alpha_g(t)-2} \right]^2 \\ &\quad - \frac{\lambda_g^2 \lambda_v^2 s A^2(t)}{4\pi} \left[\frac{\alpha'_g}{2} \frac{\Gamma\left[3 - \frac{\chi_g}{2}\right] \Gamma\left[1 - \frac{\alpha_g(t)}{2}\right]}{\Gamma\left[2 - \frac{\chi_g}{2} + \frac{\alpha_g(t)}{2}\right]} \left(\frac{\alpha'_g s}{2} \right)^{\alpha_g(t)-2} \right] \\ &\quad \times \left[\alpha'_v \sin\left(\frac{\pi\alpha_v(t)}{2}\right) (\alpha'_v s)^{\alpha_v(t)-1} \Gamma[-\alpha_v(t)] \right] \cos\left[\frac{\pi}{2}(\alpha_g(t) - \alpha_v(t))\right] \\ &\quad + \frac{\lambda_v^4}{4\pi} \left[\alpha'_v \sin\left(\frac{\pi\alpha_v(t)}{2}\right) (\alpha'_v s)^{\alpha_v(t)-1} \Gamma[-\alpha_v(t)] \right]^2, \end{aligned} \quad (11)$$

which leads to the total cross section:

$$\begin{aligned} \sigma_{\text{tot}} = & \lambda_g^2 \sin\left(\frac{\pi\alpha_g(0)}{2}\right) \frac{\Gamma\left[3 - \frac{\chi_g}{2}\right] \Gamma\left[1 - \frac{\alpha_g(t)}{2}\right]}{\Gamma\left[2 - \frac{\chi_g}{2} + \frac{\alpha_g(t)}{2}\right]} \left(\frac{\alpha'_g s}{2}\right)^{\alpha_g(0)-1} \\ & - 2\lambda_v^2 \alpha'_v \sin^2\left(\frac{\pi\alpha_v(0)}{2}\right) (\alpha'_v s)^{\alpha_v(0)-1} \Gamma[-\alpha_v(0)]. \end{aligned} \quad (12)$$

To numerically evaluate the differential cross section, the nucleon form factor $A(t)$ needs to be specified. For this we employ the gravitational form factor calculated with the bottom-up AdS/QCD model [21]. Utilizing the soft-wall model, in which the AdS geometry is smoothly cut off in the infrared region, it can be obtained as

$$A(t) = (a + 1) \left[-(1 + a + 2a^2) + 2a(1 + 2a^2)\Phi(-1, 1, a) \right], \quad (13)$$

where $\Phi(-1, 1, a)$ is the LerchPhi function, and $a = t/(8\kappa^2)$ in which κ is a parameter. κ affects the behavior of the nucleon wave function at the infrared boundary, and can be determined with the nucleon and ρ meson mass, m_n and m_ρ , following the relations: $m_n^2 = 8\kappa^2$ and $m_\rho^2 = 4\kappa^2$. Hence, this form factor does not bring any adjustable parameters into the present model setup.

III. NUMERICAL RESULTS

Here we explain how to determine the model parameters and display the numerical results. The present model involves eight parameters in total. However, for most of them we can utilize the values determined in the preceding studies, due to the universality of the Pomeron and Reggeon. All the parameter values used in this study are summarized in Table I. For the Pomeron related parameters, we utilize the values obtained in Ref. [37], in which only the Pomeron exchange contribution was taken into account to investigate the pp and $p\bar{p}$ cross sections, focusing on the high energy region. For the Reggeon related parameters, except for the Reggeon-neutron coupling λ_{vnn} , we utilize the values determined in Ref. [41], in which both the Pomeron and Reggeon contributions were considered to describe the pp and $p\bar{p}$ total cross sections in the medium energy region. Since the charge difference affects the Reggeon coupling, the Reggeon-proton and Reggeon-antiproton coupling constant, λ_{vpp} and $\lambda_{v\bar{p}\bar{p}}$, are different from each other.

Therefore, to investigate the pn and $\bar{p}n$ scattering, we only need to determine a single adjustable parameter, which is the Reggeon-neutron coupling constant λ_{vnn} . In this study,

TABLE I. Parameter values.

Parameter	Value	Source
$\alpha_g(0)$	1.084	fit to $pp(p\bar{p})$ scattering data at high energies [37]
α'_g	0.368 GeV ⁻²	fit to $pp(p\bar{p})$ scattering data at high energies [37]
λ_g	9.593 GeV ⁻¹	fit to $pp(p\bar{p})$ scattering data at high energies [37]
$\alpha_v(0)$	0.444	fit to $pp(p\bar{p})$ scattering data at medium energies [41]
α'_v	0.925 GeV ⁻²	fit to $pp(p\bar{p})$ scattering data at medium energies [41]
λ_{vpp}	7.742	fit to $pp(p\bar{p})$ scattering data at medium energies [41]
$\lambda_{v\bar{p}\bar{p}}$	16.127	fit to $pp(p\bar{p})$ scattering data at medium energies [41]
λ_{vnn}	8.088 ± 0.029	this work

this determination is done by performing a numerical fit, utilizing the MINUIT package [44] and focusing on the total cross section at $\sqrt{s} \geq 5$ GeV. Using Eq. (12) and the pn and $\bar{p}n$ total cross section data summarized by the Particle Data Group (PDG) in 2022 [45], we determine λ_{vnn} , and the resulting best fit value is shown in Table I. We display our calculations in Figs. 1 and 2. It is seen that the experimental data for both the pn and $\bar{p}n$ scattering are well described with the present model in the medium energy region, where both the Pomeron and Reggeon exchange give substantial contributions to the cross section.

Once the parameter λ_{vnn} is determined, using Eq. (11), we can predict the differential cross section without any additional parameters. Since we focus on the Regge regime and need to avoid the effect of the Coulomb interaction, similar to the previous works [37, 41], we limit the considered kinematic region to $\sqrt{s} \geq 10$ GeV and $0.01 \leq |t| \leq 0.45$ GeV², and show our predictions for the pn scattering in Fig. 3. Although the \sqrt{s} range, in which the experimental data exist, is narrow, it is found that our predictions are overall consistent with the data in the considered kinematic region. In the first two panels, there are some deviations between our predictions and the data, which may be due to the relatively low center-of-mass energies. Some deviations are also seen in the result for $\sqrt{s} = 21.471$ GeV, but our results for $\sqrt{s} = 19.416$ and 22.956 GeV are well.

As to the $\bar{p}n$ scattering, currently there are no available data with which we can compare our predictions. Hence we present the comparison between our predictions for the pn and $\bar{p}n$ scattering in Fig. 4. It is seen that the differences between the pn and $\bar{p}n$ results decrease as

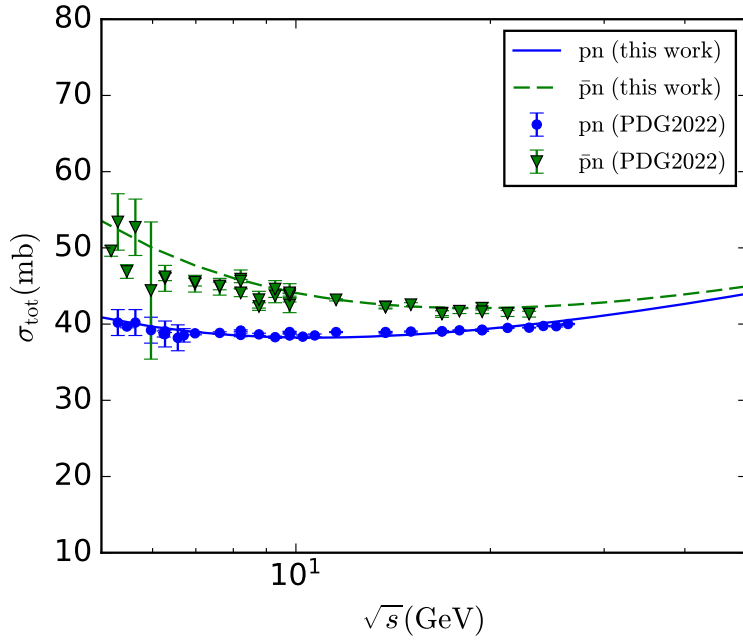


FIG. 1. The total cross section as a function of \sqrt{s} . The solid and dashed curve represent our calculations for the pn and $\bar{p}n$ scattering, respectively. The experimental data are taken from Ref. [45] and depicted with error bars.

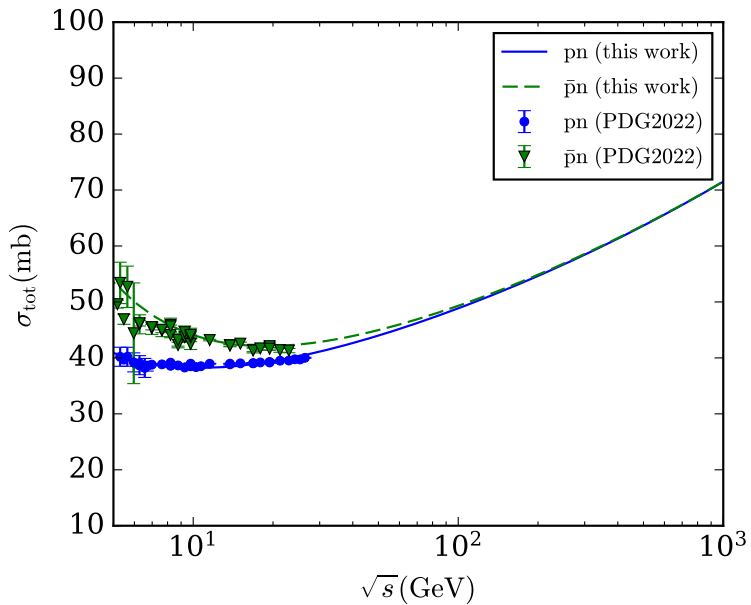


FIG. 2. Similar to Fig. 1, but for the wider \sqrt{s} range.

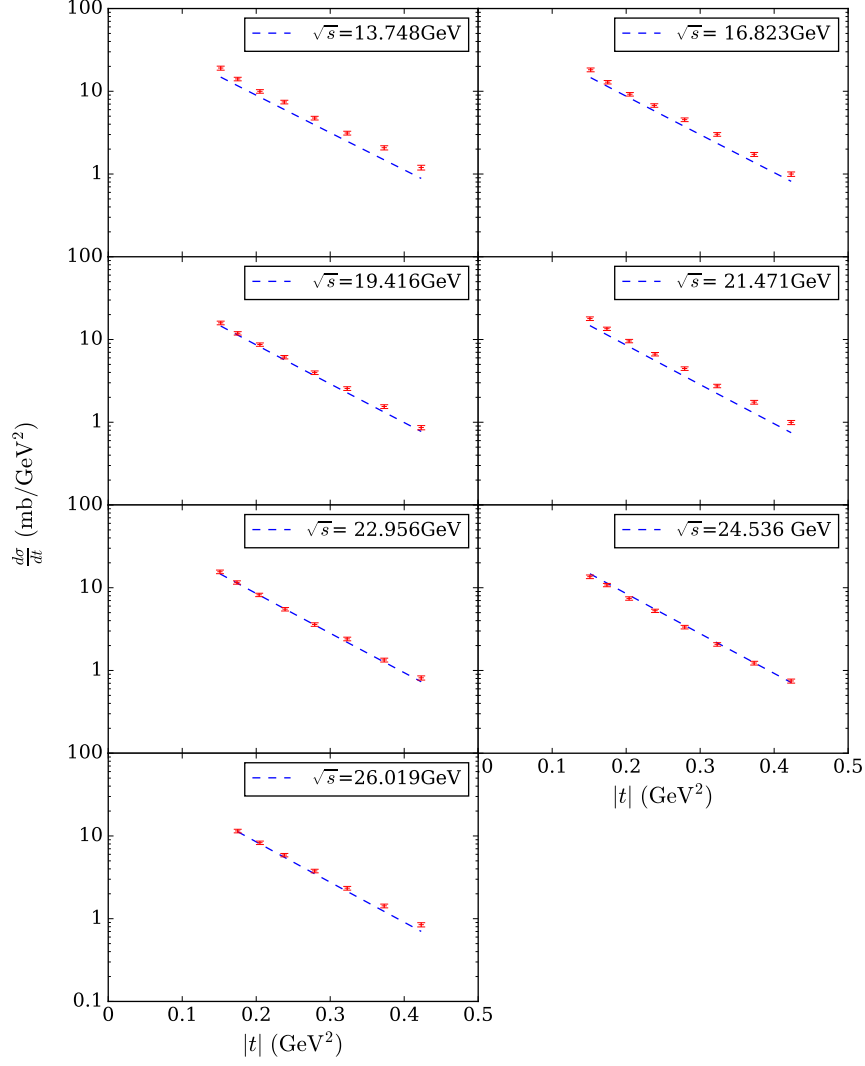


FIG. 3. The differential cross section of the pn scattering as a function of $|t|$ for various \sqrt{s} . The dashed curves represent our predictions. The experimental data are taken from Ref. [46] and depicted with error bars.

the energy increases, which reflects the fact that the Reggeon contribution decreases and the Pomeron contribution becomes dominant. At $\sqrt{s} = 50$ GeV, the both results take the almost same values. The energy dependence of the Pomeron and Reggeon exchange contribution was investigated in detail for the $pp(p\bar{p})$ scattering in Ref. [41], and our predictions are consistent with their results.

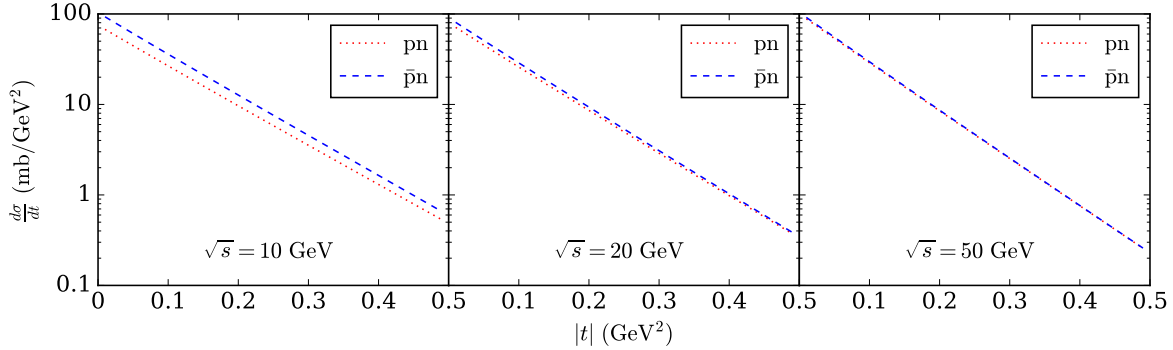


FIG. 4. The differential cross section as a function of $|t|$ for $\sqrt{s} = 10, 20,$ and 50 GeV. The dotted and dashed curves represent our predictions for the pn and $\bar{p}n$ scattering, respectively.

IV. CONCLUSION

We have investigated the elastic pn and $\bar{p}n$ scattering in a holographic QCD model, taking into account the Pomeron and Reggeon exchange in the Regge regime. In our model setup, the Pomeron and Reggeon exchange are described by the Reggeized spin-2 glueball and vector meson propagator, respectively, and for the Pomeron-nucleon coupling the nucleon gravitational form factor, which can be calculated with the bottom-up AdS/QCD model, is utilized. There are several parameters in the model, but for most of them we can employ the values determined in the preceding studies, due to the universality of the Pomeron and Reggeon. Hence we only need to determine a single parameter, which is the Reggeon-neutron coupling constant, to calculate the pn and $\bar{p}n$ cross sections.

Focusing on the total cross section, we have performed a numerical fit to determine this parameter, and found that the experimental data of both the pn and $\bar{p}n$ can be well described within the model. Once the parameter is determined, the differential cross section can be predicted without any adjustable parameters. Although the currently available data are limited, we have explicitly shown that our predictions are consistent with those, which implies the predictive ability of the present model. Further applications to other scattering processes are certainly needed. Moreover, it is expected that future experiments of high energy forward scattering will help to better constrain the model and improve our understanding of the nonperturbative nature of the strong interaction, which is one of the most important problems in high energy physics.

ACKNOWLEDGMENTS

The work of A.W. was supported by the start-up funding from China Three Gorges University. A.W. is also grateful for the support from the Chutian Scholar Program of Hubei Province.

-
- [1] S. J. Brodsky and G. R. Farrar, Scaling Laws at Large Transverse Momentum, *Phys. Rev. Lett.* **31**, 1153 (1973).
 - [2] V. A. Matveev, R. M. Muradian, and A. N. Tavkhelidze, Automodellism in the large - angle elastic scattering and structure of hadrons, *Lett. Nuovo Cim.* **7**, 719 (1973).
 - [3] G. P. Lepage and S. J. Brodsky, Exclusive Processes in Perturbative Quantum Chromodynamics, *Phys. Rev. D* **22**, 2157 (1980).
 - [4] A. Donnachie and P. V. Landshoff, Total cross-sections, *Phys. Lett. B* **296**, 227 (1992), arXiv:hep-ph/9209205.
 - [5] M. Kruczenski, D. Mateos, R. C. Myers, and D. J. Winters, Meson spectroscopy in AdS / CFT with flavor, *JHEP* **0307**, 049, arXiv:hep-th/0304032 [hep-th].
 - [6] D. T. Son and M. A. Stephanov, QCD and dimensional deconstruction, *Phys.Rev.* **D69**, 065020 (2004), arXiv:hep-ph/0304182 [hep-ph].
 - [7] M. Kruczenski, D. Mateos, R. C. Myers, and D. J. Winters, Towards a holographic dual of large $N(c)$ QCD, *JHEP* **0405**, 041, arXiv:hep-th/0311270 [hep-th].
 - [8] T. Sakai and S. Sugimoto, Low energy hadron physics in holographic QCD, *Prog. Theor. Phys.* **113**, 843 (2005), arXiv:hep-th/0412141.
 - [9] J. Erlich, E. Katz, D. T. Son, and M. A. Stephanov, QCD and a holographic model of hadrons, *Phys. Rev. Lett.* **95**, 261602 (2005), arXiv:hep-ph/0501128.
 - [10] T. Sakai and S. Sugimoto, More on a holographic dual of QCD, *Prog.Theor.Phys.* **114**, 1083 (2005), arXiv:hep-th/0507073 [hep-th].
 - [11] L. Da Rold and A. Pomarol, Chiral symmetry breaking from five dimensional spaces, *Nucl.Phys.* **B721**, 79 (2005), arXiv:hep-ph/0501218 [hep-ph].
 - [12] S. J. Brodsky, G. F. de Teramond, H. G. Dosch, and J. Erlich, Light-Front Holographic QCD and Emerging Confinement, *Phys. Rept.* **584**, 1 (2015), arXiv:1407.8131 [hep-ph].

- [13] J. M. Maldacena, The Large N limit of superconformal field theories and supergravity, *Adv. Theor. Math. Phys.* **2**, 231 (1998), arXiv:hep-th/9711200.
- [14] S. S. Gubser, I. R. Klebanov, and A. M. Polyakov, Gauge theory correlators from noncritical string theory, *Phys. Lett. B* **428**, 105 (1998), arXiv:hep-th/9802109.
- [15] E. Witten, Anti-de Sitter space and holography, *Adv. Theor. Math. Phys.* **2**, 253 (1998), arXiv:hep-th/9802150.
- [16] G. F. de Teramond and S. J. Brodsky, Hadronic spectrum of a holographic dual of QCD, *Phys. Rev. Lett.* **94**, 201601 (2005), arXiv:hep-th/0501022.
- [17] A. Karch, E. Katz, D. T. Son, and M. A. Stephanov, Linear confinement and AdS/QCD, *Phys. Rev. D* **74**, 015005 (2006), arXiv:hep-ph/0602229.
- [18] S. J. Brodsky and G. F. de Teramond, Light-Front Dynamics and AdS/QCD Correspondence: The Pion Form Factor in the Space- and Time-Like Regions, *Phys. Rev. D* **77**, 056007 (2008), arXiv:0707.3859 [hep-ph].
- [19] Z. Abidin and C. E. Carlson, Gravitational form factors of vector mesons in an AdS/QCD model, *Phys. Rev. D* **77**, 095007 (2008), arXiv:0801.3839 [hep-ph].
- [20] Z. Abidin and C. E. Carlson, Gravitational Form Factors in the Axial Sector from an AdS/QCD Model, *Phys. Rev. D* **77**, 115021 (2008), arXiv:0804.0214 [hep-ph].
- [21] Z. Abidin and C. E. Carlson, Nucleon electromagnetic and gravitational form factors from holography, *Phys. Rev. D* **79**, 115003 (2009), arXiv:0903.4818 [hep-ph].
- [22] T. Branz, T. Gutsche, V. E. Lyubovitskij, I. Schmidt, and A. Vega, Light and heavy mesons in a soft-wall holographic approach, *Phys. Rev. D* **82**, 074022 (2010), arXiv:1008.0268 [hep-ph].
- [23] T. Gutsche, V. E. Lyubovitskij, I. Schmidt, and A. Vega, Dilaton in a soft-wall holographic approach to mesons and baryons, *Phys. Rev. D* **85**, 076003 (2012), arXiv:1108.0346 [hep-ph].
- [24] D. Li and M. Huang, Dynamical holographic QCD model for glueball and light meson spectra, *JHEP* **11**, 088, arXiv:1303.6929 [hep-ph].
- [25] T. Gutsche, V. E. Lyubovitskij, and I. Schmidt, Electromagnetic structure of nucleon and Roper in soft-wall AdS/QCD, *Phys. Rev. D* **97**, 054011 (2018), arXiv:1712.08410 [hep-ph].
- [26] V. E. Lyubovitskij and I. Schmidt, Nucleon resonances with higher spins in soft-wall AdS/QCD, *Phys. Rev. D* **102**, 094008 (2020), arXiv:2009.07115 [hep-ph].
- [27] J. Polchinski and M. J. Strassler, Hard scattering and gauge / string duality, *Phys. Rev. Lett.* **88**, 031601 (2002), arXiv:hep-th/0109174.

- [28] J. Polchinski and M. J. Strassler, Deep inelastic scattering and gauge / string duality, JHEP **05**, 012, arXiv:hep-th/0209211.
- [29] R. C. Brower, J. Polchinski, M. J. Strassler, and C.-I. Tan, The Pomeron and gauge/string duality, JHEP **12**, 005, arXiv:hep-th/0603115.
- [30] Y. Hatta, E. Iancu, and A. H. Mueller, Deep inelastic scattering at strong coupling from gauge/string duality: The Saturation line, JHEP **01**, 026, arXiv:0710.2148 [hep-th].
- [31] B. Pire, C. Roiesnel, L. Szymanowski, and S. Wallon, On AdS/QCD correspondence and the partonic picture of deep inelastic scattering, Phys. Lett. B **670**, 84 (2008), arXiv:0805.4346 [hep-ph].
- [32] C. Marquet, C. Roiesnel, and S. Wallon, Virtual Compton Scattering off a Spinless Target in AdS/QCD, JHEP **04**, 051, arXiv:1002.0566 [hep-ph].
- [33] A. Watanabe and K. Suzuki, Transition from soft- to hard-Pomeron in the structure functions of hadrons at small- x from holography, Phys. Rev. D **86**, 035011 (2012), arXiv:1206.0910 [hep-ph].
- [34] A. Watanabe and K. Suzuki, Nucleon structure functions at small x via the Pomeron exchange in AdS space with a soft infrared wall, Phys. Rev. D **89**, 115015 (2014), arXiv:1312.7114 [hep-ph].
- [35] A. Watanabe and H.-n. Li, Photon structure functions at small x in holographic QCD, Phys. Lett. B **751**, 321 (2015), arXiv:1502.03894 [hep-ph].
- [36] A. Watanabe and M. Huang, Total hadronic cross sections at high energies in holographic QCD, Phys. Lett. B **788**, 256 (2019), arXiv:1809.02515 [hep-ph].
- [37] W. Xie, A. Watanabe, and M. Huang, Elastic proton-proton scattering at LHC energies in holographic QCD, JHEP **10**, 053, arXiv:1901.09564 [hep-ph].
- [38] P. Burikham and D. Samart, Open-string singlet interaction as pomeron in elastic $pp, p\bar{p}$ scattering, Eur. Phys. J. C **79**, 452 (2019), arXiv:1902.05706 [hep-ph].
- [39] A. Watanabe, T. Sawada, and M. Huang, Extraction of gluon distributions from structure functions at small x in holographic QCD, Phys. Lett. B **805**, 135470 (2020), arXiv:1910.10008 [hep-ph].
- [40] Z. Liu, W. Xie, F. Sun, S. Li, and A. Watanabe, Elastic pion-proton and pion-pion scattering at high energies in holographic QCD, Phys. Rev. D **106**, 054025 (2022), arXiv:2202.08013 [hep-ph].

- [41] Z. Liu, W. Xie, and A. Watanabe, Pomeron and Reggeon contributions to elastic proton-proton and proton-antiproton scattering in holographic QCD, *Phys. Rev. D* **107**, 014018 (2023), arXiv:2210.11246 [hep-ph].
- [42] M. Yamada, THE PROPAGATOR OF A MASSIVE SPIN 3 FIELD, *Phys. Rev. D* **30**, 2144 (1984).
- [43] N. Anderson, S. Domokos, and N. Mann, Central production of η via double Pomeron exchange and double Reggeon exchange in the Sakai-Sugimoto model, *Phys. Rev. D* **96**, 046002 (2017), arXiv:1612.07457 [hep-ph].
- [44] F. James and M. Roos, Minuit: A System for Function Minimization and Analysis of the Parameter Errors and Correlations, *Comput. Phys. Commun.* **10**, 343 (1975).
- [45] R. L. Workman *et al.* (Particle Data Group), Review of Particle Physics, *PTEP* **2022**, 083C01 (2022).
- [46] C. E. DeHaven, Jr., C. A. Ayre, H. R. Gustafson, L. W. Jones, M. J. Longo, P. V. Ramana Murthy, T. J. Roberts, and M. R. Whalley, NEUTRON - PROTON DIFFERENTIAL CROSS-SECTIONS AT FERMILAB ENERGIES, FERMILAB-PUB-78-117-E, UM-HE-78-30 (1978).